Surface functionalization of gold nanoparticles using hetero-bifunctional poly(ethylene glycol) spacer for intracellular tracking and delivery

Dinesh Shenoy[1]
Wei Fu[2]
Jane Li[3]
Curtis Crasto[3]
Graham Jones[3]
Charles DiMarzio[4]
Srinivas Sridhar[2]
Mansoor Amiji[1]

Departments of [1]Pharmaceutical Sciences, [2]Physics, [3]Chemistry and Chemical Biology, [4]Electrical and Computer Engineering, and the Nanomedicine Consortium, Northeastern University, Boston, MA, USA

Abstract: For the development of surface-functionalized gold nanoparticles as cellular probes and delivery agents, we have synthesized hetero-bifunctional poly(ethylene glycol) (PEG, MW 1500) having a thiol group on one terminus and a reactive functional group on the other for use as a flexible spacer. Coumarin, a model fluorescent dye, was conjugated to one end of the PEG spacer and gold nanoparticles were modified with coumarin-PEG-thiol. Surface attachment of coumarin through the PEG spacer decreased the fluorescence quenching effect of gold nanoparticles. The results of cellular cytotoxicity and fluorescence confocal analyses showed that the PEG spacer-modified nanoparticles were essentially non-toxic and could be efficiently internalized in the cells within 1 hour of incubation. Intracellular particle tracking using a Keck 3-D Fusion Microscope System showed that the functionalized gold nanoparticles were rapidly internalized in the cells and localized in the peri-nuclear region. Using the PEG spacer, the gold nano-platform can be conjugated with a variety of biologically relevant ligands such as fluorescent dyes, antibodies, etc in order to target, probe, and induce a stimulus at the target site.

Keywords: gold nanoparticles, hetero-bifunctional poly(ethylene glycol) spacer, surface functionalization, cellular trafficking, cytotoxicity

Introduction

Nanotechnology is expected to revolutionize medicine. A variety of medical processes occur at nanometer length scales. Among the approaches for exploiting developments in nanotechnology in medicine, nanoparticles offer some unique advantages as sensing, delivery, and image-enhancement agents (West and Halas 2000; LaVan et al 2002). Several varieties of nanoparticles are available (Sahoo and Labhasetwar 2003): polymeric nanoparticles, dendrimers, metal nanoparticles, quantum dots, liposomes, micelles, and other types of nano-assemblies. All of these nanostructures can play a major role in medicine, and especially in disease diagnosis and therapy.

Rapid advances in molecular biology and genetic engineering provide an unprecedented opportunity for delivery of drugs and genes to intracellular targets (Torchilin and Lukyanov 2003). In cancer, for instance, the effectiveness of many anticancer drugs and genes is limited due to the inability to reach the target site in sufficient concentrations and exert the pharmacological effect. Current intracellular delivery systems are classified as being either viral or non-viral in origin. Viruses are efficient in delivery; however, they suffer from poor safety profiles (Marshall 2000; Check 2002). Non-viral delivery systems, albeit not as efficient as viruses, have the promise of safety and reproducibility in manufacturing (Nishikawa and Hashida 2002).

Correspondence: Mansoor Amiji
Department of Pharmaceutical Sciences, Northeastern University, 360 Huntington Avenue, Boston, MA 02115, USA
Tel +1 617 373 3137
Fax +1 617 373 8886
Email m.amiji@neu.edu

To enhance delivery of drugs and genes to intracellular targets using non-viral delivery systems, it is necessary to have a detailed understanding of the transport process and identify ways of overcoming the cellular barriers (Kaneda 2004).

Nanoparticles based on gold chemistry have attracted significant research and practical attention recently. They are versatile agents with a variety of biomedical applications including use in highly sensitive diagnostic assays (Goodman et al 2004), thermal ablation, and radiotherapy enhancement (Hirsch et al 2003; Hainfeld et al 2004), as well as for drug and gene delivery (Thomas and Klibanov 2003). For instance, antibody-modified gold nanoparticles, when used for detection of prostate-specific antigen, had an almost million-fold higher sensitivity than conventional ELISA-based assays (Nam et al 2003). Near-infrared-radiation-absorbing gold–silica nanoshells have been prepared and evaluated for thermal ablation of tumors after systemic administration (O'Neal et al 2004).

For biomedical applications, surface functionalization of gold nanoparticles is essential to apply them to specific disease areas and allow them to selectively interact with cells or biomolecules. Surface conjugation of antibodies and other targeting moieties is usually achieved by adsorption of the ligand to the gold surface. Surface adsorption, however, can denature the proteins or, in some cases, limit the interactions of the ligand with the target on the cell surface due to steric hinderance. Additionally, for systemic applications, long-circulating nanoparticles are desired for passive targeting to tumors and inflammatory sites. Poly(ethylene glycol) (PEG) modification of nanoparticles affords a long-circulating property by evading macrophage-mediated uptake and removal from the systemic circulation (Kommareddy and Amiji 2004). Surface modification of gold nanoparticles through the PEG spacer would, therefore, allow the modified nanoparticles to remain in the systemic circulation for the prolonged period and provide flexibility to the attached ligand for efficient interaction with its target.

In the present study, we describe the synthesis and characterization of hetero-bifunctional PEG with a thiol group on one terminus and a reactive functional group on the other for conjugation to a biologically relevant targeting moiety. Using thiol-PEG-coumarin, a model fluorescent dye, we describe the "proof-of-concept" for surface functionalization of gold nanoparticles, cellular cytotoxicity evaluations, and fluorescence confocal analysis of cell uptake and nanoparticle distribution.

Experimental procedures

Synthesis and characterization of coumarin-PEG-thiol

A versatile hetero-bifunctional PEG compound containing end-groups of thiol and alcohol derivatized as the coumarin carbamate was efficiently prepared as shown in Figure 1. The key step for the PEG synthesis involves the desymmetrization of the PEG-diol compound. This was achieved by monotosylation of the PEG-diol (Aldrich, Milwaukee, WI, USA) using the method of Bouzide and Sauve (2002).

Synthesis of derivative (1)

To a chilled (0 °C) solution of the PEG (M_w = 1427 g/mol, 12.0 g; 8.40 mmol) in methylene chloride (distilled, 250 mL) was added freshly prepared Ag_2O (1.50 equiv, 2.92 g; 12.6 mmol) and recrystallized potassium iodide (0.40 equiv, 558 mg; 3.36 mmol). To this rapidly stirred solution in one portion, purified tosyl chloride (TsCl) (1.05 equiv, 1.68 g; 8.82 mmol) was added. The reaction was deemed to be complete in 1–2 hours by TLC (alumina). This was done by UV monitoring of the consumption of the TsCl reagent and the appearance of the tosylate product as a weakly UV active compound. The mixture was then carefully filtered over a pad of celite, and the clear filtrate obtained was then evaporated under reduced pressure to give a colorless oily product. Trituration with portions of ether to remove any trace TsCl reagent, followed by recrystallization (acetone/dry-ice bath) using methylene chloride–ether mixture, provided the monotosyl-PEG derivative as a white amorphous solid. Yield: 12.5 g (95%); ^{1}H NMR ($CDCl_3$, 300 MHz) δ7.80 (d, J = 8.1 Hz, Ar), 7.35 (d, J = 8.1 Hz, Ar), 4.16 (t, $\underline{CH_2}OTs$), 3.86–3.39 (m, 29 × CH_2), 3.43 (t, 2H, CH_2), 2.83 (t, 2H, CH_2), 2.63 (br, s, OH), 2.45 (s, M*e tosyl*); ^{13}C NMR ($CDCl_3$, MHz) δ143.95, 132.41, 129.10, 127.12, 125.4, 71.85, 69.74, 69.49, 68.60, 67.83, 60.66, 20.83 ($\underline{Me}SO_2$); IR (υ, cm^{-1}) 3620–3192 (br, m), 2879 (br, vs), 1646, 1598, 1468, 1358 (asymmetric SO_2 stretch), 1279, 1234, 1145 (symmetric SO_2 stretch), 1112 (br, vs), 945, 927, 840; ESIMS calculated for $MH^+ + H_2O$ (0.81) *m/z* 1598.95, found 1598.91.

Synthesis of derivative (2)

A solution of the monotosyl-PEG (12.0 g; 7.59 mmol), 10 equiv of potassium thioacetate (8.67 g; 75.9 mmol) in dry MeOH (300 mL) was heated to reflux for 48 hours under an atmosphere of nitrogen. The solution was allowed to cool

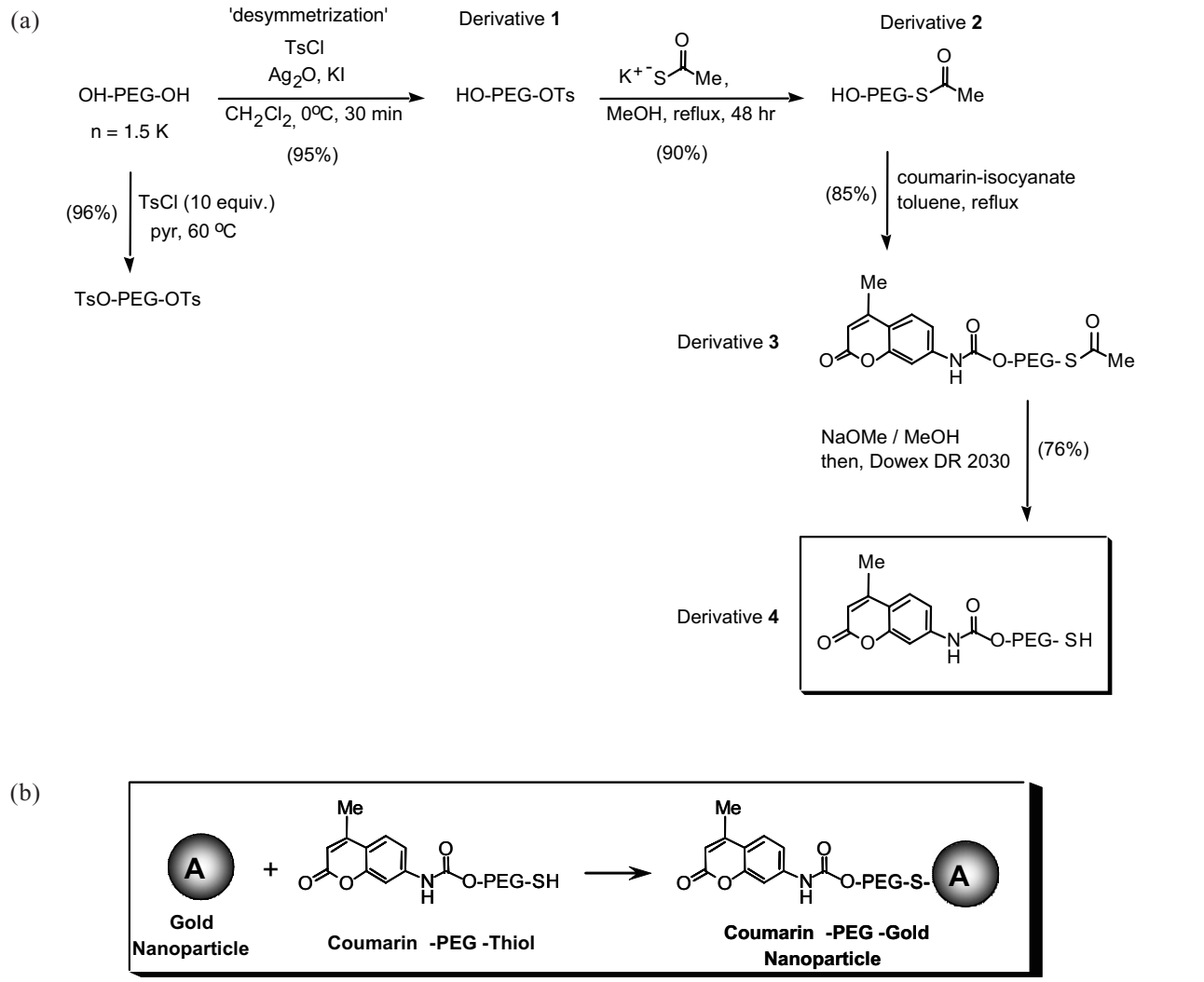

Figure 1 Schematic illustration for the chemical synthesis of hetero-bifunctional poly(ethylene glycol) having a thiol group on one terminus and coumarin carbamate on the other for attachment to gold nanoparticles (a) and surface functionalization of gold nanoparticles with coumarin-poly(ethylene glycol)-thiol (b).

to room temperature, and the MeOH removed using a Buchi rotary evaporator. The solid reaction mixture was treated with methylene chloride and the solution filtered. Concentration under reduced pressure gave the crude product, which was purified by chromatography using alumina and by eluting with 1% acetic acid/1% MeOH in methylene chloride. This purification yielded the product as a pale-yellow oil; and crystallization using ether (dry ice/acetone bath) provided the PEG thioacetate derivative as a pale-yellow solid. Yield: 10.1 g (90%); ^{1}H NMR ($CDCl_3$, 300 MHz) δ4.18 (t, 2H, CH_2), 3.94–3.62 (m, 58H, 29 × CH_2), 3.41 (t, 2H, CH_2), 2.83 (m, 2H, CH_2), 2.81 (br s, 1H, OH), 2.04 (s, 3H, S<u>Ac</u>); ^{13}C NMR ($CDCl_3$, MHz) δ227.78 (SC[O]), 72.12, 70.05, 69.83, 69.21, 61.04, 28.33 (SC[O]<u>Me</u>); IR (υ, cm^{-1}) 3603–3277 (br, m), 2888 (br, vs), 1697, 1466, 1359, 1347, 1277, 1242, 1112 (br, vs), 1061 (s, SO stretch), 948, 842; MALDI calculated for $M+Na^{+}+H_2O$ (1.67) *m/z* 1538.90, found 1538.88.

Synthesis of derivative (3)

To a solution of the monothioacetate-PEG (2.50 g; 1.68 mmol) in toluene (70 mL) was added freshly prepared coumarin isocyanate (1.05 equiv, 355 mg; 76 mmol). The solution was heated to reflux for 12 hours under an atmosphere of nitrogen. Then, the mixture was allowed to cool and the toluene was removed using a Buchi rotary evaporator. The crude product mixture was then treated with methylene chloride and the solution filtered over a pad of celite. Evaporation of the filtrate followed and then purification using alumina, by eluting with 1%–2% MeOH

in methylene chloride), gave the product as a pale-yellow oil. Finally, crystallization using ether (dry ice/acetone bath) provided the coumarin-PEG-thioacetate derivative as a pale-yellow solid. Yield: 2.41 g (85%); ^{1}H NMR ($CDCl_3$, 300 MHz) δ7.87 (br s, 1H, NH), 7.53–7.41 (m, 3H, Ar), 6.17 (s, 1H, vinyl), 4.20 (t, 2H, CH_2), 3.87–3.40 (m, 60H, $30 \times CH_2$), 2.83 (m, 2H, CH_2), 2.40 (s, 3H, vinyl Me), 2.08 (s, 3H, SAc); ^{13}C NMR ($CDCl_3$, MHz) δ227.48,0020160.15, 153.59, 152.55, 151.64, 141.82, 124.33, 114.07, 113.92, 111.81, 104.97, 71.83, 70.03, 69.71, 69.57, 68.50, 63.42, 60.71, 29.14 (SC[O]Me), 17.76 (Me); IR (υ, cm^{-1}) 3558.04 (w), 2870 (s), 1732 (C=O, carbamate), 1694, 1620, 1575, 1533, 1463, 1350, 1291, 1231, 1108, 943; MALDI calcd, for $M + Na^+ + H_2O$ (2.45) *m/z* 1754.13, found 1754.15.

Synthesis of derivative (4)

A solution of the bifunctional coumarin-PEG-thioacetate compound (0.50 g; 0.30 mmol) in degassed methanol (50 mL) was treated with 5 equivalents of degassed 0.5 M NaOMe/MeOH. The mixture was allowed to stir overnight at room temperature. Then, the mixture was acidified using DOWEX-DR 2030 resin to pH 1–2. The solution was quickly filtered over an overhead stream of nitrogen, and the solvent was removed using a rotary evaporator to give the crude product. Purification by silica gel chromatography and by eluting with 2%–6% MeOH in methylene chloride gave the coumarin-PEG-thiol bifunctional derivative, which was obtained as a light-yellow solid upon further drying under diminished pressure. Yield: 375 mg (76%); ^{1}H NMR ($CDCl_3$, 300 MHz) δ8.0 (br s, 1H, NH), 7.52–7.42 (m, 3H, Ar), 6.17 (s, 1H, vinyl), 4.35 (t, 2H, CH_2), 3.94–3.63 (m, 58H, $29 \times CH_2$), 3.50 (t, 2H, CH_2), 2.83 (m, 2H, CH_2), 2.41 (s, 3H, vinyl Me), 1.25 (br s, 1H, SH); ^{13}C NMR ($CDCl_3$, MHz) δ227.48, 160.15, 153.62, 152.58, 151.64, 141.85, 124.34, 114.09, 113.96, 111.82, 104.99, 71.82, 70.05, 69.76, 69.55, 68.51, 63.43, 60.69, 29.53, 17.74; IR (υ, cm^{-1}) 3421 (br, vs), 2918 (SH, m), 2882, 1651, 1463, 1351, 1297, 1251, 1100, 949; MALDI calculated for $M + Na^+ + H_2O$ (3.99) *m/z* 1739.84, found 1739.91.

Preparation and characterization of coumarin-PEG-functionalized gold nanoparticles

Gold nanoparticles were synthesized by reduction of gold chloride ($HAuCl_4$) with freshly prepared sodium citrate and allowed to boil under reflux conditions (Daniel and Astruc 2004). The pale-yellow solution turned to deep red as the gold nanoparticles were formed and stabilized by adsorbed citrate ions. Particle size analysis was performed with a Coulter® N-4 sub-micron particle size analyzer (Coulter Corporation, Miami, FL, USA). The nanoparticle suspension was air-dried on the specimen grid and observed with a transmission electron microscope (TEM).

Coumarin-PEG-thiol was added to the aqueous dispersion of gold nanoparticles and the reaction for conjugation of the fluorescence dye to the gold surface through the thiol functionality was carried out at room temperature. The coumarin dye was used primarily as a demonstration of the covalent attachment, and confirms two important issues. First, because of the covalent bonding, the fluorescence observed is not from detached dye molecules, but from the fluorescent entity covalently attached to the gold nanoparticles. Second, the fluorescence is not quenched by the presence of the gold nanoparticles, probably due to the presence of the PEG spacer.

Cytotoxicity studies

The in vitro cytotoxicity of the coumarin-PEG-thiol functionalized gold nanoparticles was measured using a commercially available CellTiter 96® AQueous Non-Radioactive Cell Proliferation Assay kit (Promega Corporation, Madison, WI, USA). According to the manufacturer's instructions, the tetrazolium compound (3-[4,5-dimethylthiazol-2-yl]-5-[3-carboxy-methoxyphenyl]-2-[4-sulfophenyl]-2H- tetrazolium, [MTS]) is bioreduced by viable cells into a formazan product. Approximately 10 000 MDA-MB-231 human breast carcinoma xenograft cells, suspended in Dulbecco's minimum essential medium (DMEM) modified with 10% (v/v) fetal bovine serum and other essential nutrients, were seeded per well into 96-well plates and allowed to adhere for 24 hours at 37 °C and 5% CO_2 atmosphere. The medium was then replaced with graded concentrations of poly-ethyleneimine (MW ~ 10000) as a positive control; unfunctionalized gold nanoparticles and nanoparticles functionalized with methoxy-PEG-thiol (OMe-PEG-SH) as negative controls; and gold nanoparticles functionalized with coumarin-PEG-thiol as the test preparation in serum-free medium (SFM). Incubation then continued for another 24 hours. Additional control wells received only SFM. After the incubation time, the cells were washed once with sterile phosphate-buffered saline (PBS, pH 7.4), followed by the addition of 180 µl of DMEM per well. The plates were incubated for 4 hours after the addition of 20 µl of MTS solution to each well and the absorbance of the formed formazan product was read at 490 nm using a microplate

reader. The absorbance values were converted to the percentage viability against control and reported as mean and standard deviation.

Intracellular trafficking studies using Keck 3-D Fusion microscope system

The Keck 3-D Fusion microscope system was developed at Northeastern University based on a commercially available Nikon TE2000U inverted microscope. It has 5 different modes of operation on one common platform: quadrature microscopy (QM); differential interference contrast (DIC); confocal fluorescence microscopy (CFM); 2-photon confocal laser scanning microscopy with second-harmonic generation (2PM); and confocal reflectance microscopy (CRM).

A known number of cells were grown on circular glass cover slips in a 6-well plate containing DMEM. Once they had reached suitable confluency, the medium was replaced with SFM and the controls and test preparations were added. The final concentration of coumarin-PEG-thiol functionalized gold nanoparticles was 100 μg/mL per well and the samples were incubated for 1 hour. The cells were washed with sterile PBS twice and fixed with a para-formaldehyde solution (0.5% [w/v] in PBS). The cover slips were mounted (with cell side down) onto clean glass slides using Fluoromount G mounting medium. The fluorescent images were registered using an in-house built Keck 3-D Fusion microscope system using a 100× oil immersion objective.

We used the 2-photon laser scanning microscopy to measure the fluorescent signatures of coumarin-PEG-gold nanoparticles in the cells. The sample slide was placed on the stage with sample side down. The immersion oil was required for the objective. The tunable titanium–sapphire laser was set to 780 nm for illumination. Detection was completed with a sensitive head-on photo multiplier tube (PMT) (HC1024-02, Hamamatsu).

Results and discussion

In the present study, we have synthesized hetero-bifunctional PEG having a thiol group on one terminus and an alcohol carbamate on the other for covalent attachment of coumarin. The PEG derivative was synthesized in high efficiency and characterized during each step of the synthesis pathway. Surface functionalization through PEG spacers would allow for flexibility in the attached molecule for more efficient interactions with the biological target. Otsuka et al (2001) reported on the synthesis of hetero-bifunctional PEG synthesis having acetal-PEG-SH functionalities for attachment of lactose and other sugar molecules. They have also evaluated the interactions of the surface-attached sugar residues on gold nanoparticles with specific lectins for the development of biosensors.

As shown by the Coulter particle-size analysis results in Figure 2, we can reproducibly prepare 10–15 nm gold nanoparticles with a narrow size distribution. A TEM image shows that the nanoparticles have a spherical shape. The surface of gold nanoparticles was functionalized with coumarin-PEG-thiol by a covalent conjugation reaction. The unbound coumarin-PEG-thiol was removed by multiple centrifugation and washing steps, and the emission from bound dye was measured with a fluorescence spectro-photometer. Although gold nanoparticles are known to be very efficient fluorescence quenchers (Fan et al 2003), the attachment of coumarin through PEG spacers did show significant emission intensity. The PEG-modified gold nanoparticles (with methoxy-PEG-thiol and coumarin-PEG thiol) did not aggregate even in high-ionic-strength solutions, confirming that the stable surface presence of PEG was effective in steric repulsion of the gold nanoparticles.

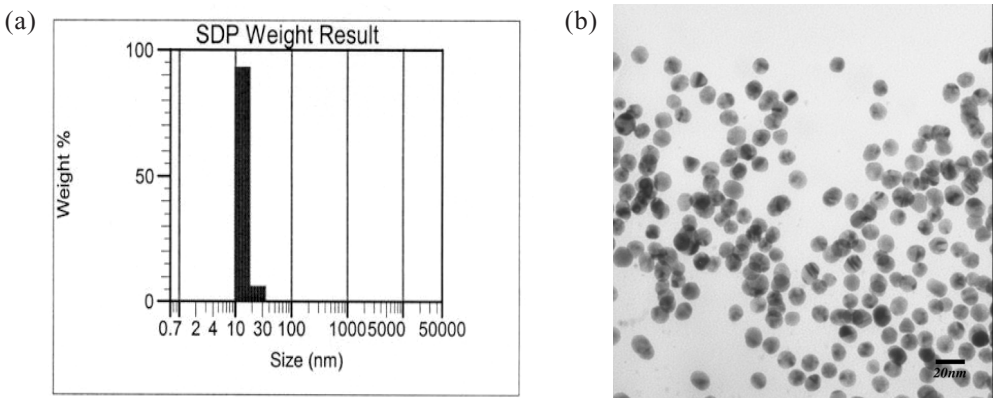

Figure 2 Coulter particle-size analysis (a) and transmission electron microscopy image of gold nanoparticles (b). Scale bar in (b) = 20 nm.

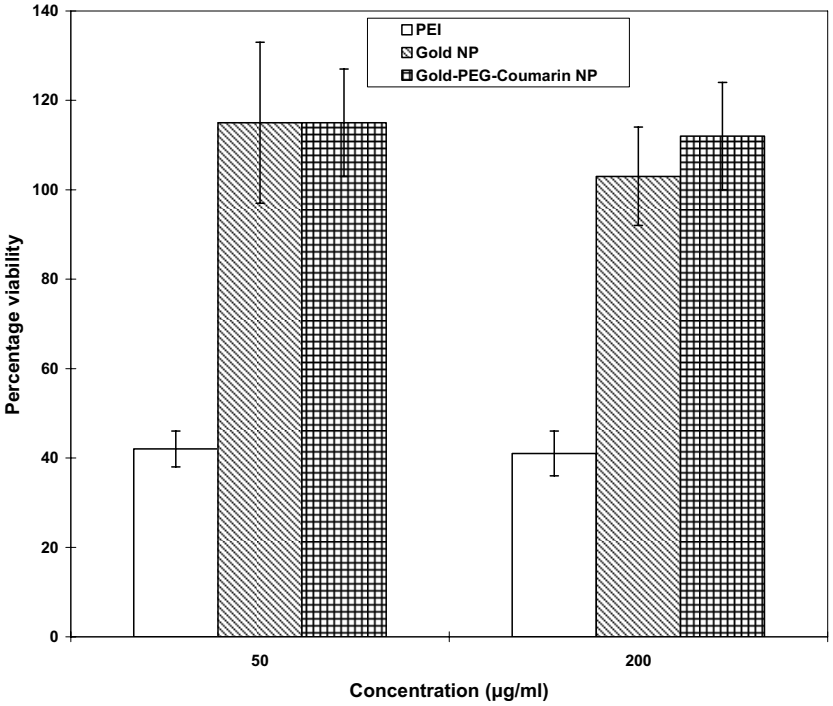

Figure 3 Cytotoxicity analysis of the controls and coumarin-poly(ethylene glycol)-thiol functionalized gold nanoparticles in MDA-MB-231 human breast adenocarcinoma cells. Bare gold nanoparticles were used as a negative control and polyethyleneimine (MW 10 000) was used as a positive control.

Cellular cytotoxicity studies in Figure 3 show that gold nanoparticles, gold nanoparticles functionalized with methoxy-PEG-thiol (ie, gold-PEG-OMe nanoparticles), and coumarin-PEG-thiol functionalized gold nanoparticles were not cytotoxic at the concentrations studied. In contrast, polyethyleneimine (PEI), a known cytotoxic compound, did reduce cell viability to 40% of the control at the same concentrations.

As shown in Figure 4, upon incubation with MDA-MB-231 cells in culture, the coumarin-PEG-thiol functionalized gold nanoparticles were internalized by non-specific endocytosis within the first few minutes. Within 30 minutes, a large fraction of the administered dose was found to be in the early endosomes. As time progressed, the nanoparticles traversed through the cytosol and reached the perinuclear region within 1 hour of incubation. The hetero-bifunctional PEG derivative with a molecular weight of 1500 daltons was sufficient to allow flexibility in the attached fluorescent ligand, but did not prevent cellular entry of the nanoparticles. In addition, we did not observe any of the gold nanoparticles inside the nucleus even after 24 hours of incubation. Several recent studies, including some from our group (Kaul and Amiji 2005), have shown that when nanoparticles are internalized in cells through endocytotic process, they tend to converge to the perinuclear area. Suh et al (2003) attributed this directed intracellular movement of nanocarriers as an active transport process driven by molecular motor proteins. Using the Keck 3-D Fusion microscope system, fast data acquisition, and custom particle tracking software, we can track functionalized gold nanoparticles inside the cells.

Conclusions

Gold nanoparticle surfaces were functionalized with coumarin, a fluorescent dye, through PEG spacers and used for intracellular tracking in MDA-MB-231 cells. Using the Keck 3-D Fusion microscope system, we can track functionalized nanoparticles with nanometer accuracy. The results show that these nanoparticles were rapidly internalized in the cells through non-specific endocytotic pathways and were found in the perinuclear region within 1 hour of incubation. Using the PEG spacer, the gold nanoplatform can be conjugated with a variety of stimuli (eg, cell-penetrating peptides, endosomal buffering agents), probes (eg, radiolabel, fluorescent dye), and moieties to study cellular transport pathways and barriers to efficient gene transfection.

Acknowledgments

This study was supported by a grant RO1-CA095522 from the National Cancer Institute of the National Institutes of Health and by the Electronic Materials Research Institute of Northeastern University.

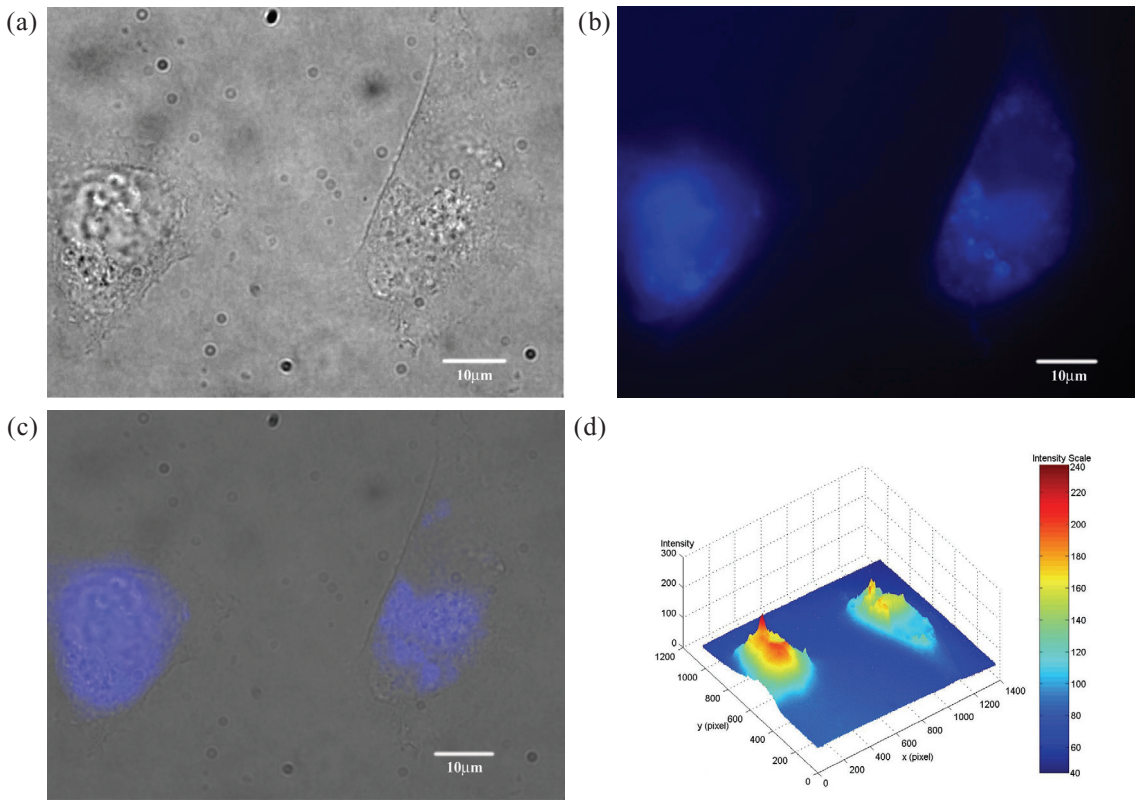

Figure 4 Cellular uptake and distribution of coumarin-poly(ethylene glycol)-thiol functionalized gold nanoparticles in MDA-MB-231 human breast adenocarcinoma cells. Differential interference contrast (a), epifluorescence (b), merged images (c), and 3D plot of fluorescence intensity distribution as a function of the X and Y coordinates was plotted (d). Original magnification was 100×. Scale bars in (a)–(c) = 10 μm.

References

Bouzide A, Sauve G. 2002. Silver(I) oxide mediated highly selective monotosylation of symmetrical diols. Application to the synthesis of polysubstituted cyclic ethers. *Org Lett*, 4:2329–32.

Check E. 2002. Gene therapy: a tragic setback. *Nature*, 420:116–18.

Daniel M-C, Astruc D. 2004. Gold nanoparticles: assembly, supramolecular chemistry, quantum-size-related properties, and applications toward biology, catalysis, and nanotechnology. *Chem Rev*, 104:293–346.

Fan C, Wang S, Hong JW, et al. 2003. Beyond superquenching: hyper-efficient energy transfer from conjugated polymers to gold nanoparticles. *Proc Natl Acad Sci U S A*, 100:6297–301.

Goodman CM, McCusker CD, Yilmaz T, et al. 2004. Toxicity of gold nanoparticles functionalized with cationic and anionic side chains. *Bioconjug Chem*, 15:897–900.

Hainfeld JF, Slatkin DN, Smilowitz HM. 2004. The use of gold nanoparticles to enhance radiotherapy in mice. *Phys Med Biol*, 49: N309–15.

Hirsch LR, Stafford RJ, Bankson JA, et al. 2003. Nanoshell-mediated near-infrared thermal therapy of tumors under magnetic resonance guidance. *Proc Natl Acad Sci U S A*, 100:13549–54.

Kaneda Y. 2004. Biological barriers to gene transfer. In Amiji MM (ed). Polymeric gene delivery: principles and applications, Chapter 3. Boca Raton, FL: CRC Press, LLC. p 29–41.

Kaul G, Amiji M. 2005. Cellular interactions and in vitro DNA transfection studies with poly(ethylene glycol)-modified gelatin nanoparticles. *J Pharm Sci*, 94:184–98.

Kommareddy S, Amiji M. 2004. Targeted drug delivery to tumor cells using colloidal carriers. In Lu DR, Oie S (eds). Cellular drug delivery: principles and practice, Chapter 10. Totowa: Humana Pr. p 181–215.

LaVan DA, Lynn DM, Langer R. 2002. Moving smaller in drug discovery and delivery. *Nat Rev Drug Discov*, 1:77–84.

Marshall E. 2000. Gene therapy on trial. *Science*, 288:951–6.

Nam J-M, Thaxton CS, Mirkin CA. 2003. Nanoparticle-based bio-bar codes for the ultrasensitive detection of proteins. *Science*, 301:1884–7.

Nishikawa M, Hashida M. 2002. Nonviral approaches satisfying various requirements for effective in vivo gene therapy. *Biol Pharm Bull*, 25:275–83.

O'Neal DP, Hirsch LR, Halas NJ, et al. 2004. Photo-thermal tumor ablation in mice using near infrared-absorbing nanoparticles. *Cancer Lett*, 209:171–6.

Otsuka H, Akiyama Y, Nagasaki Y, 2001. Quantitative and reversible lectin-induced association of gold nanoparticles modified with a-lactosyl-w-mercapto-poly(ethylene glycol). *J Am Chem Soc*, 123:8226–30.

Sahoo SK, Labhasetwar V. 2003. Nanotech approaches to drug delivery and imaging. *Drug Discov Today*, 8:1112–20.

Suh J, Wirtz D, Hanes J. 2003. Effective active transport of gene nanocarriers to the cell nucleus. *Proc Natl Acad Sci U S A*, 100: 3878–82.

Thomas M, Klibanov A. 2003. *Proc Natl Acad Sci U S A*, 100:9138–43.

Torchilin VP, Lukyanov A. 2003. Peptide and protein drug delivery to and into tumors: challenges and solutions. *Drug Discov Today*, 8:259.

West JL, Halas NJ. 2000. Applications of nanotechnology to biotechnology commentary. *Curr Opin Biotechnol*, 11:215–17.